Influence of Adipose Tissue Distribution, Sarcopenia, and Nutritional Status on Clinical Outcomes After CD19 CAR T-cell Therapy

Kai Rejeski[1,2,3], David M. Cordas dos Santos[1,3,4], Nathan H. Parker[5], Veit L. Bücklein[1,2], Michael Winkelmann[6], Khushali S. Jhaveri[5], Lian Liu[7], Paul Trinkner[1,4], Sophie Günther[1,4], Philipp Karschnia[8], Viktoria Blumenberg[1,2,3], Christian Schmidt[1], Wolfgang G. Kunz[6], Michael von Bergwelt-Baildon[1,3,7], Michael D. Jain[5], Sebastian Theurich[1,3,4], and Marion Subklewe[1,2,3]

ABSTRACT

Although CD19-directed chimeric antigen receptor T-cell therapy (CD19.CAR-T) has proven clinical efficacy for multiple refractory B-cell malignancies, over 50% of patients ultimately relapse. Recent evidence has underlined the critical role of the host in determining treatment responses. In this retrospective observational study of 106 patients with relapsed/refractory large B-cell lymphoma receiving standard-of-care CD19.CAR-T, we analyzed the impact of immunometabolic host features and detailed body composition measurements on post–CAR T clinical outcomes. We extracted muscle and adipose tissue distributions from prelymphodepletion CT images and assessed laboratory-based immuno-nutritional scores. Early responders displayed increased total abdominal adipose tissue deposits (TAT: 336 mm^3 vs. 266 mm^3, $P = 0.008$) and favorable immuno-nutritional scores compared to nonresponding patients. On univariate Cox regression analysis, visceral fat distribution, sarcopenia, and nutritional indices significantly impacted both progression-free (PFS) and overall survival (OS). Patients with a low skeletal muscle index (SMI; e.g.<34.5), a sarcopenia indicator, exhibited poor clinical outcomes (mOS 3.0 months vs. 17.6 months, log-rank $P = 0.0026$). Prognostically adverse immuno-nutritional scores were linked to inferior survival [low PNI: HR_{OS}, 6.31; 95% confidence interval (CI), 3.35–11.90; $P < 0.001$]. In a multivariable analysis adjusting for baseline Eastern Cooperative Oncology Group performance status, C-reactive protein, and lactate dehydrogenase, increased TAT was independently associated with improved clinical outcomes (adjusted HR_{OS}, 0.27; 95% CI, 0.08–0.90; $P = 0.03$). We noted particularly favorable treatment outcomes in patients with both increased abdominal fat and muscle mass (TAT^{high}/SMI^{high}: 1-year PFS 50%, 1-year OS 83%). These real-world data provide evidence for a role of body composition and immuno-nutritional status in the context of CD19.CAR-T and suggest that the obesity paradox may extend to modern T cell–based immunotherapies.

See related Spotlight by Nawas and Scordo, p. 704

Introduction

CD19 CAR T-cell therapy (CD19.CAR-T) has emerged as a practice-changing immunotherapy for a range of refractory B-cell malignancies (1–5). Still, a significant proportion of CAR T–treated patients ultimately relapse (6, 7), and identifying novel determinants of treatment response would help to refine response prediction tools and optimize patient selection. Risk factors for treatment outcomes of CD19.CAR-T can broadly be divided into disease-specific and host-intrinsic factors. Established disease-specific and local risk factors include *TP53* mutational status, low target antigen expression levels, and an immuno-hostile tumor microenvironment that negatively influences CAR T-cell expansion and persistence (8–10). On the other hand, recent evidence has highlighted the critical role of systemic host factors in driving responses to CD19.CAR-T. For example, healthy hematopoiesis and gut microbiome composition have been linked to improved treatment responses (11–13). Although other host-intrinsic features, such as nutritional status, body weight, and muscle mass, have been extensively studied across different cancer treatment modalities, their prognostic influence in cell therapy patients is less clear.

Being overweight and/or obese has repeatedly been proven to be an adverse risk factor in the context of chemotherapy and classic oncologic procedures like radiotherapy and surgical resection (14, 15). However, the last decades of immunotherapy has interestingly shown an unexpected relationship between excess adipose tissue and immunotherapy efficacy, a phenomenon aptly coined the "obesity paradox" (16). This clinical observation is well-described for immune checkpoint blockade both in preclinical models and in patients with cancer (17, 18). The therapeutic benefit in the excess weight population was especially pronounced in patients who developed immune-related adverse events (19). The impact of being overweight

[1]Department of Medicine III, University Hospital, Ludwig Maximilian University (LMU) Munich, Munich, Germany. [2]Laboratory for Translational Cancer Immunology, LMU Gene Center, Munich, Germany. [3]German Cancer Consortium (DKTK), Munich Site, and German Cancer Research Center, Heidelberg, Germany. [4]Cancer and Immunometabolism Research Group, LMU Gene Center, Munich, Germany. [5]Department of Blood and Marrow Transplant and Cellular Immunotherapy, Moffitt Cancer Center, Tampa, Florida. [6]Department of Radiology, University Hospital, LMU Munich, Munich, Germany. [7]Comprehensive Cancer Center Munich, LMU Munich, Munich, Germany. [8]Department of Neurosurgery, University Hospital, LMU Munich, Munich, Germany.

K. Rejeski, D.M. Cordas dos Santos, S. Theurich, and M. Subklewe contributed equally to this article.

Corresponding Authors: Marion Subklewe, Department of Medicine III - Hematology/Oncology, University Hospital, LMU Munich, Munich, 81377, Germany. E-mail: marion.subklewe@med.uni-muenchen.de; and Sebastian Theurich, Cancer and Immunometabolism Research Group, LMU Gene Center, Feodor-Lynen-Straße 35, 81377 Munich, Germany. E-mail: Sebastian.theurich@med.uni-muenchen.de

Cancer Immunol Res 2023;11:707–19

doi: 10.1158/2326-6066.CIR-22-0487

and/or obese on survival in patients with B-NHL treated in the pre–CAR T era has been mixed, with heterogenous study results (20–22). A potential explanation for the superior survival of overweight patients undergoing immunotherapy is the immunogenic function of adipose tissue. An excess of adipose tissue is associated with systemic low-grade inflammation in a process termed "metaflammation," wherein adipose tissue is transformed into an inflammatory endocrine organ with the ability to secrete pro-inflammatory cytokines (e.g., IL6, TNFα, and IL1β) due to the infiltration of M1-polarized macrophages, T cells, and other immune cells (23). Importantly, body mass index (BMI) represents only a vague measure of obesity and does not reflect effects of specific adipose tissue sites (e.g., VAT, visceral; EAT, epicardial; SAT, subcutaneous), which can exert distinct effects on the degree of metaflammation and differentially influence obesity-associated diseases (24). In patients receiving CD19.CAR-T, we recently demonstrated that visceral adipose tissue, in particular, is asociated with the onset and severity of cytokine release syndrome (CRS) via IL6 (25).

Next to adipose tissue distribution, the amount and functionality of muscle mass is critical in patients with cancer who are at high risk for muscle loss, termed sarcopenia, due to a combination of malnutrition, inflammation, and cachexia (26). Sarcopenia is accompanied with poorer quality of life, more severe chemotherapeutic toxicity, and adverse clinical outcomes (27). Moreover, the immunomodulatory role of skeletal muscle as a potential integrator between sarcopenia and immune senescence has been recognized more recently (27, 28). Pathomechanistically, skeletal muscle cells can signal through cell surface molecules, cell-to-cell interactions, and muscle cell–derived cytokines, termed myokines, which can broadly modulate the immune system (29, 30). To understand the intersection of diet and host systemic inflammatory responses, immuno-nutritional scores have been developed that often incorporate serum albumin levels and inflammatory markers such as C-reactive protein (CRP) or leucocyte subsets (31–37). Scores that have been validated in patients undergoing classical cancer treatments include the Glasgow prognostic score (GPS; refs. 31, 32), CRP-to-albumin ratio (33), prognostic nutritional index (PNI; ref. 34), and neutrophil-to-lymphocyte ratio (NLR; ref. 35). Nutritional status has also been actively discussed as a potential influencing factor of CAR T-cell expansion and function (38).

Overall, a growing body of evidence points towards the multifunctional role of adipose and muscle tissue in shaping the response to modern immunotherapies. However, the specific impact of body composition on clinical outcomes after CD19.CAR-T remains poorly understood and insufficiently addressed. Here, we comprehensively report the prognostic role of adipose tissue distribution, sarcopenia, and nutritional status on early response and survival outcomes after CD19.CAR-T in patients with relapsed/refractory large B-cell lymphoma (R/R LBCL).

Materials and Methods

Patient cohort

We included all patients with available anthropometric measurements and CT-based segmentation analyses receiving CD19.CAR-T for R/R LBCL at the Ludwig-Maximilians-University (LMU) Hospital and Moffitt Cancer Center between December 2017 and March 2022 (data cutoff; **Fig. 1A**). Patients were treated with axicabtagene ciloleucel (Axi-cel) or tisagenlecleucel (Tisa-cel) in a standard-of-care setting. Clinical trial participation ($n = 7$) and CAR-T treatment for a disease entity other than R/R LBCL ($n = 18$) represented the key exclusion criteria, resulting in a final study population of 106 patients, including 100 patients with available baseline imaging. Lymphodepleting chemotherapy with fludarabine (Axi-cel: 30 mg/m^2 i.v., Tisa-cel: 25 mg/m^2 i.v.) and cyclophosphamide (Axi-cel: 500 mg/m^2 i.v., Tisa-cel: 250 mg/m^2 i.v.) was administered prior to CAR-T transfusion according to the manufacturers' instructions (1, 2). CRS and ICANS were graded according to American Society for Transplantation and Cellular Therapy (ASTCT) consensus criteria (39). High-grade CRS and ICANS were defined as ASTCT grade ≥3 toxicity. Toxicity management followed institutional guidelines, as described previously (25). Clinical metadata were obtained with institutional review board approval (LMU Ethics Committee, Project No. 19–817). The study was conducted in accordance with the Declaration of Helsinki, and informed written consent was provided.

Data collection and body composition measurements

Baseline serum laboratory markers were determined prior to lymphodepletion (e.g., day −5) with a leniency period of up to 3 days. Measurements were performed according to clinical standard procedures in the Department of Laboratory Medicine of the involved hospitals. Results were extracted from the patient's medical records.

Body composition measurements were extracted from clinical records (weight, height) or prelymphodepletion CT scans (waist, adipose/muscle tissue distribution). The following anthropometric measures were considered: BMI, waist circumference (waist), and waist-to-height ratio (WtHR; **Fig. 1A**, middle). Single chest CT slices were utilized to derive waist measurements using ImageJ (v2.0; ref. 40). To quantify adipose (e.g., SAT, VAT) and muscle tissue distribution (psoas and skeletal muscle), we performed segmentation analyses of single CT slices at lumbar spine 3 using the Slice-O-Matic software package (v5.0, Tomovision). Cross-sectional areas of respective tissues were computed for each image. Total abdominal adipose tissue (TAT) was determined as the sum of VAT and SAT. To calculate muscle indices [psoas muscle index (PMI); skeletal muscle index (SMI)], the mean muscle area was divided by height. EAT content was quantified by calculating the mean EAT amount at the bottom, middle (4-chamber view), and top (left main coronary artery view) of the heart, as described previously (25). Adipose and muscle tissue discrimination was based on predefined Hounsfield units (HU) ranges [−190 to −30 HU for SAT, −150 to −50 HU for VAT, −190 to −30 HU for EAT, −29 to +150 HU for PM/SM (40–42)].

Immuno-nutritional scores were calculated on the basis of the extracted laboratory markers (Supplementary Table S1). The GPS was based on a combination of CRP and albumin levels: CRP ≤10 mg/L was scored as 0, CRP > 10 mg/L and albumin > 3.5 g/dL were scored as 1, and CRP > 10 mg/L and albumin < 3.5 g/dL were scored as 2 (31, 32). The CRP-to-albumin ratio was calculated by dividing CRP (mg/L) by albumin (g/dL ref. 33). The PNI was calculated using the following formula: albumin (g/dL) + 0.005 × total lymphocyte count (per mm^3; ref. 34). The neutrophil-to-lymphocyte ratio was calculated by dividing the absolute neutrophil count (per mm^3) by the total lymphocyte count (per mm^3; ref. 35).

Clinical outcomes

Efficacy outcomes were assessed according to Lugano criteria (43). Best response at day 90 was defined as reaching at least a partial remission (PR) or better, whereas nonresponders exhibited stable disease (SD) or progressive disease (PD), or deceased due to treatment-related causes (44). Nonrelapse mortality was defined as death after cellular therapy without prior relapse or progression. Kaplan–Meier estimates for progression-free (PFS) and overall survival (OS) were assessed from time of CAR-T transfusion, and groups were

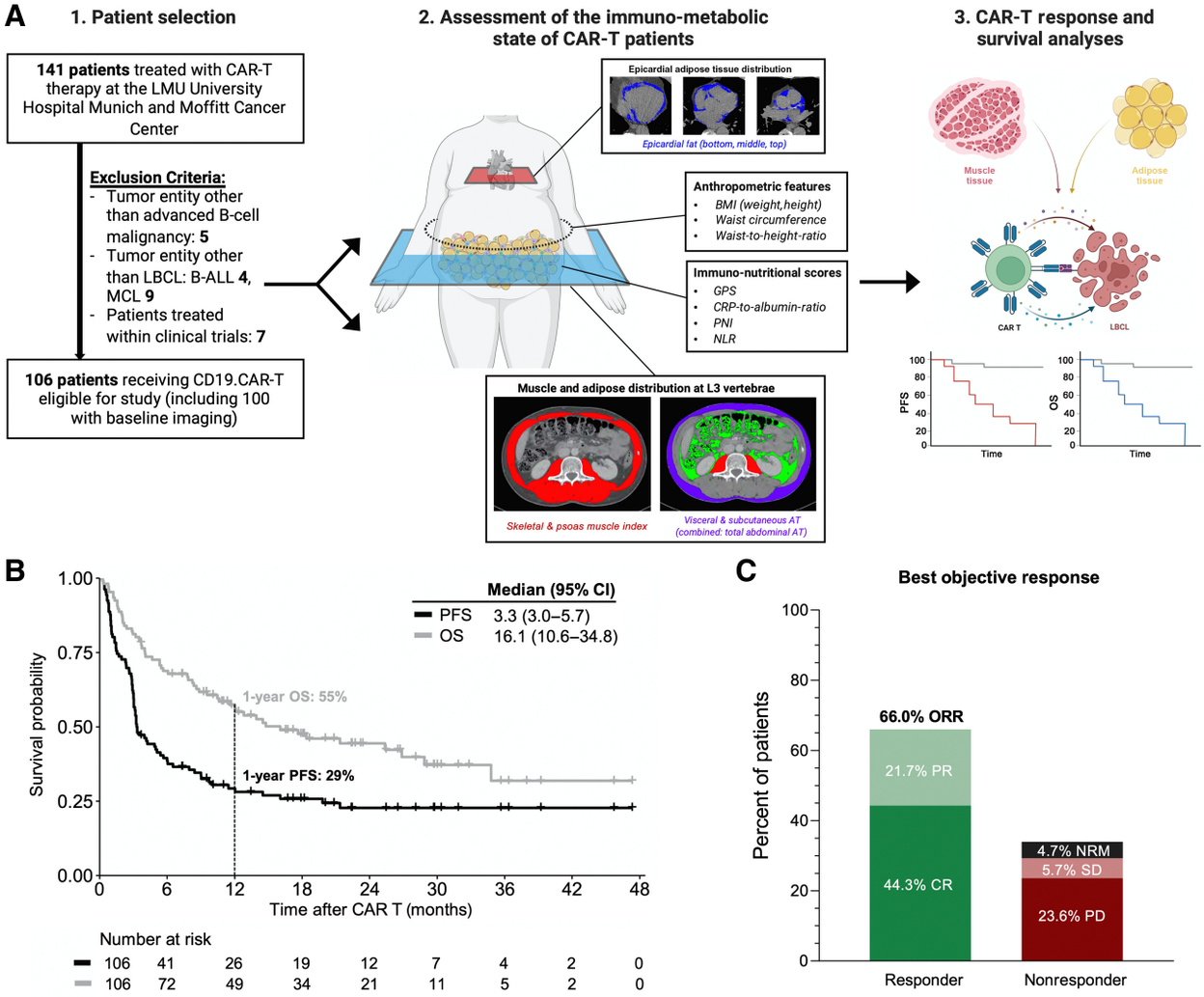

Figure 1.

The study cohort exhibits representative real-world clinical outcomes. **A,** Schema outlining from 1 to 3 (left to right): The study cohort with key exclusion criteria, methods of body composition measurements and assessment of the patient-individual immunometabolic state, and the study endpoints. **B,** Kaplan-Meier estimates of PFS (dark gray) and OS (light gray) for the entire study cohort ($n = 106$). Median survival in months and 1-year survival are depicted. **C,** Best objective response rate (ORR) at day 90 as determined according to Lugano criteria. Abbreviations: CR, complete remission; PR, partial remission; SD, stable disease; PD, progressive disease; NRM, nonrelapse mortality.

compared using the log-rank test. Follow-up was calculated from CAR-T transfusion until death from any cause or last time of contact.

Statistical considerations

Mann–Whitney test or Student *t* test were used to explore continuous variables, whereas Fisher exact test and χ^2 test were used to study categorical variables. The d'Agostino Pearson test was used to determine normal distribution. If not stated otherwise, continuous variables were reported as median and interquartile range (IQR). Associations between continuous variables were analyzed using the Spearman correlation coefficient (*r*). Bonferroni correction was performed to account for multiple comparisons. Cutoffs were derived using a survival-based software package fitting a Cox proportional hazard model (45). To study the prognostic impact of the different body composition parameters, we performed univariate and multivariable Cox Regression for survival outcomes (PFS/OS). A log transformation using base 2 (log2) or 10 (log10) was applied to covariates to reduce skewness. The multivariable analysis was adjusted for established adverse risk factors of CD19.CAR-T (6, 10), which exhibited a *P*-value <0.1 on univariate analysis [e.g., log10 lactate dehydrogenase (LDH), log10 CRP, Eastern Cooperative Oncology Group (ECOG) performance status ≥2]. TAT and SMI were introduced into the multivariable models as log-transformed continuous variables. Statistical analysis and data visualization were performed using GraphPad Prism (v9.0), SPSS (IBM, v26.0), and R Statistical Software (v4.1.0).

Data availability

For all original data and material, please contact the corresponding authors.

Results

Patient characteristics

Clinical outcomes were assessed in 106 patients with R/R LBCL treated with CD19.CAR-T in a standard-of-care setting (**Table 1**; **Fig. 1A**). The applied CAR product was axicabtagene ciloleucel in 68 patients (64%) and tisagenlecleucel in 38 patients (36%). The most common disease subtype was LBCL, NOS (64%), followed by lymphoma transformed from indolent B-NHL (33%) and primary mediastinal large B-cell lymphoma (PMBCL; 3%). Patients received a median of three prior treatment lines (excluding bridging), which included autologous or allogeneic stem cell transplantation in 31 (29%) and 4 (4%) patients, respectively. In terms of immunotoxicity, we observed 20 patients (19%) with high-grade ICANS and 10 patients (9.4%) with high-grade CRS (Supplementary Table S1). Glucocorticoids were applied in 48 patients (45%). After a median follow-up time of 22.7 months, median PFS and OS were 3.3 and 16.1 months, respectively (**Fig. 1B**). With a 1-year PFS and OS of 29% and 55%, survival was comparable with previous real-world reports (6). Of note, survival outcomes did not significantly differ by participating center (Supplementary Fig. S1). The best 90-day overall response rate was 66%, with a complete remission rate of 44% (**Fig. 1C**). The cumulative 1-year nonrelapse mortality was 3.9% (two infections, one ICANS, one CRS; Supplementary Fig. S2). When comparing responders versus nonresponders at day 90 after CD19.CAR-T, we observed increased ECOG performance status in the nonresponding patients ($P = 0.013$, **Table 1**). They also displayed significantly higher levels of systemic inflammation, as reflected by higher baseline CRP (1.9 mg/dL vs. 0.6 mg/dL, $P = 0.004$). Furthermore, serum LDH was elevated in nonresponding patients (359 U/L vs. 259 U/L, $P = 0.006$), as was the radiographic tumor load (median STL 172 mL vs. 72 mL, $P = 0.03$). Of note, high-dose glucocorticoid administration was equally distributed between CAR-T responders versus nonresponders.

Poor CD19.CAR-T responders at day 90 display reduced visceral adipose tissue and altered immuno-nutritional scores

On the basis of prelymphodepletion imaging studies, we next compared body composition features according to best response at day 90. No significant difference in BMI was observed by response ($P = 0.19$, Supplementary Table S2), consistent with prior reports (22). Other anthropometric measures, such as waist circumference and WtHR, also did not significantly differ between responding and nonresponding patients (Supplementary Fig. S3A). However, comprehensive analysis of adipose tissue distribution revealed significantly increased visceral (VAT) and total abdominal (TAT) fat deposits in responding patients, with a trend towards increased epicardial (EAT) fat deposits in evaluable patients (Supplementary Table S2). For example, the measured volumetries for VAT and TAT were 134.4 cm^2 versus 105.5 cm^2 ($P = 0.03$) and 335.7 cm^2 versus 266.3 cm^2 ($P = 0.008$) in responding versus nonresponding patients, respectively (Supplementary Fig. S3B). Furthermore, we noted a trend towards higher subcutaneous fat deposits in day 90 responders (191.1 cm^2 vs. 157.0 cm^2, $P = 0.06$). None of the sarcopenia indices (PMI, SMI) differed by the early 3-month response assessment (Supplementary Fig. S3C). Next, we studied previously established immuno-nutritional scores (e.g., GPS, CRP-to-albumin ratio, PNI, NLR), which are summarized in Supplementary Table S3. We found that CAR nonresponders displayed higher GPS scores (≥1 vs. 0: 38% vs. 10%, $P = 0.002$), higher CRP-to-albumin ratio (0.48 vs. 0.17, $P = 0.006$) and lower PNI (39.5 vs. 42.6, $P < 0.001$), whereas no significant difference in NLR was observed (Supplementary Fig. S3D). Together these findings indicate that visceral adipose tissue, nutritional status, and inflammation may be of prognostic value for early response to CD19.CAR-T.

Table 1. Baseline patient characteristics.

Characteristic	All patients ($N = 106$)	Responders ($N = 53$)	Nonresponders[a] ($N = 53$)	*P* value
Basic data				
Age in years [median (range)]	64 (19–83)	64 (36–83)	63 (19–80)	0.14
ECOG performance status (median, IQR)	1 (1–2)	1 (0–1)	1 (1–2)	**0.013**
Sex (female), *n* (%)	40 (38)	22 (42)	18 (34)	0.55
Lines of prior therapy excl. bridging (median, IQR)	3 (2–4)	2 (2–4)	3 (2–4)	0.14
Prior SCT				
Autologous SCT, *n* (%)	31 (209)	11 (21)	20 (38)	0.12
Allogeneic SCT, *n* (%)	4 (4)	3 (6)	1 (2)	
CAR product	38 (36)	20 (38%)	18 (34)	0.84
Disease subtype				
LBCL	68 (64)	29 (55)	39 (73)	**0.07**
Transformed lymphoma	35 (33)	23 (43)	12 (23)	
PMBCL	3 (3)	1 (2)	2 (4)	
Costimulatory domain				
4–1BB, *n* (%)	38 (36)	20 (38)	18 (34)	0.84
CD28z, *n* (%)	68 (64)	33 (62)	35 (66)	
Baseline laboratory values and radiographic tumor load				
CRP (mg/dL) (median, IQR)	1.23 (0.29–4.3)	0.6 (0.19–3.10)	1.9 (0.69–5.68)	**0.004**
LDH (U/L) (median, IQR)	296 (209–4)	259 (194–347)	359 (232–607)	**0.006**
STL (mL) (median, IQR)	131 (26–330)	72 (12–276)	172 (48–399)	**0.03**

Abbreviations: SCT, stem cell transplantation; STL, sum of target lesions.
[a]Patients with non-relapse mortality (NRM) events prior to the day 90 response assessment were allocated to the nonresponding group ($n = 4$). Values are shown as number (percent) if not stated otherwise. *P* values <0.1 are highlighted in bold.

Increased adipose tissue deposits are associated with favorable survival outcomes after CD19.CAR-T

Upon cutoff analysis, we identified three distinct risk groups (e.g., low, intermediate, high) for the adipose tissue markers TAT, VAT, and SAT, whereas two risk groups (high vs. low) were defined for PMI and SMI (high vs. low; Supplementary Fig. S4). On univariate Cox regression, we did not observe an association between increased BMI (defined as BMI ≥25 kg/m^2 according to WHO criteria) and survival outcomes (**Table 2**). However, increased TAT >464 cm^2 was associated with a significantly lower risk of poor PFS [HR, 0.43; 95% confidence interval (CI), 0.22–0.84; $P = 0.01$] and OS (HR, 0.29; 95% CI, 0.11–0.69; $P = 0.005$; **Table 2**). On Kaplan–Meier analysis, we noted superior survival outcomes in the patients with high levels of abdominal fat (>464 cm^2), whereas the patients with the lowest levels of abdominal fat (<293 cm^2) exhibited poor survival following CD19.CAR-T (**Fig. 2A**). When comparing TAT risk groups (high vs. intermediate vs. low), median PFS was 11.8 months versus 3.7 months versus 3.0 months (log-rank $P = 0.015$), whereas median OS was not-reached versus 28.9 months versus 10.6 months (log-rank $P = 0.0036$), respectively. These survival advantages extended to the patients with excess subcutaneous (**Fig. 2B**) and visceral adipose tissue (**Fig. 2C**). Concomitantly, increased subcutanous fat deposits were associated with a decreased risk for poor survival outcomes (HR_{PFS}, 0.68; 95% CI, 0.51–0.92; HR_{OS}, 0.59; 95% CI, 0.41–0.85). Similarly, we noted significantly improved OS in the patients with increased VAT (HR_{OS}, 0.60; 95% CI, 0.40–0.89), with a trend towards improved PFS (HR_{PFS}, 0.75; 95% CI, 0.53–1.05). Of interest, the

Table 2. Univariate Cox regression for PFS and OS.

		PFS		OS	
	N	**HR (95% CI)**	***P* value**	**HR (95% CI)**	***P* value**
Demographic and laboratory features					
ECOG performance status		2.24	**0.001**	2.28	**0.003**
≥2	28/106	(1.38–3.66)		(1.32–3.94)	
0–1 (Ref.)	78/106				
Log10 LDH (U/L)	106	3.84 (1.73–8.49)	<**0.001**	4.86 (1.89–12.52)	**0.001**
Log10 CRP (mg/dL)	106	1.48 (1.08–2.04)	**0.015**	1.26 (0.86–1.84)	0.23
Log10 STL (mL)	98	1.48 (1.06–2.07)	**0.02**	1.35 (0.92–1.99)	0.13
Anthropometric measures					
BMI		0.85 (0.54–1.32)	0.46	0.79 (0.47–1.33)	0.37
≥25 (kg/m^2)	48/106				
<25 (kg/m^2) (Ref.)	58/106				
Adipose tissue distribution					
TAT			**0.043**		**0.01**
<293 (cm^2) (Ref.)	52/100	—		—	
293–464 (cm^2)	30/100	0.72 (0.44–1.20)	0.21	0.62 (0.35–1.12)	0.11
>464 (cm^2)	18/100	0.43 (0.22–0.84)	**0.014**	0.29 (0.11–0.69)	**0.005**
SAT			**0.037**		**0.016**
<166.6 (cm^2) (Ref.)	49/100	—		—	
166.6–252 (cm^2)	31/100	0.85 (0.51–1.41)	0.53	0.52 (0.28–0.97)	**0.04**
>252 (cm^2)	20/100	0.43 (0.22–0.82)	**0.01**	0.37 (0.17–0.81)	**0.01**
VAT			0.25		**0.048**
<61.8 (cm^2) (Ref.)	21/100	—		—	
61.8–190.4 (cm^2)	56/100	0.82 (0.46–1.46)	0.50	0.64 (0.34–1.21)	0.16
>190.4 (cm^2)	23/100	0.56 (0.28–1.13)	**0.10**	0.36 (0.16–0.81)	**0.01**
Sarcopenia indices					
PMI		1.38 (0.77–2.47)	0.24	1.94 (1.02–3.69)	**0.044**
≥4.7 (cm^2/m^2) (Ref.)	82/100				
<4.7 (cm^2/m^2)	18/100				
SMI		1.88 (0.89–3.91)	**0.09**	3.29 (1.45–7.49)	**0.004**
≥34.5 (cm^2/m^2) (Ref.)	90/100				
<34.5 (cm^2/m^2)	10/100				
Immuno-nutritional scores					
GPS		3.00 (1.81–5.00)	<**0.001**	5.85 (3.26–10.52)	<**0.001**
0 (Ref.)	77/102				
1–2	25/102				
CRP-to-albumin ratio		2.66 (1.58–4.46)	<**0.001**	3.59 (2.00–6.43)	<**0.001**
≥1.44	20/102				
<1.44 (Ref.)	82/102				
PNI		3.95 (2.18–7.18)	<**0.001**	6.31 (3.35–11.90)	<**0.001**
<33.5	16/103				
≥33.5 (Ref.)	87/103				

Note: Cutoff values for waist were 88 cm for female and 102 cm for male patients. The respective reference group of the Cox regression is depicted. The T/S/VAT risk groups were treated as categorical variables, and the respective hazard ratio in relation to the reference is provided. *P* values <0.1 are highlighted in bold.
Abbreviations: E/S/V/TAT, epicardial/subcutaneous/visceral/total abdominal adipose tissue; P/SMI, psoas/skeletal muscle index; WtHR, waist-to-height ratio.

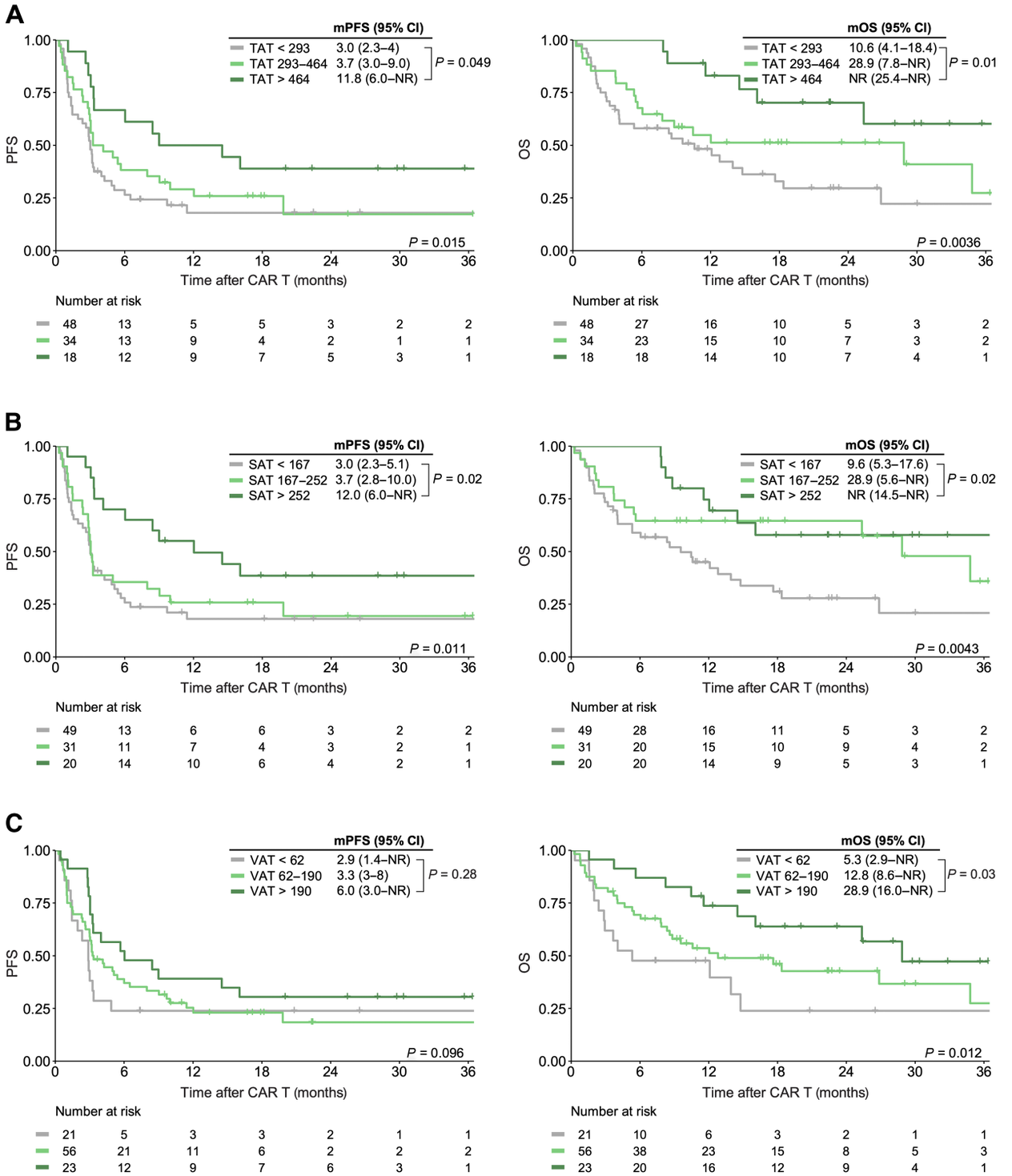

Figure 2.

Increased visceral and subcutaneous adipose tissue deposits are associated with superior PFS and OS. Kaplan–Meier estimates of median PFS (left) and OS (right) stratified by total (TAT; **A**), subcutaneous (SAT; **B**), and visceral (VAT; **C**) tissue deposits. The respective cutoff for each parameter and median survival in months is depicted above the graph. The *P* value of the Mantel–Cox log-rank test is denoted on the graph inset. NR, not reached.

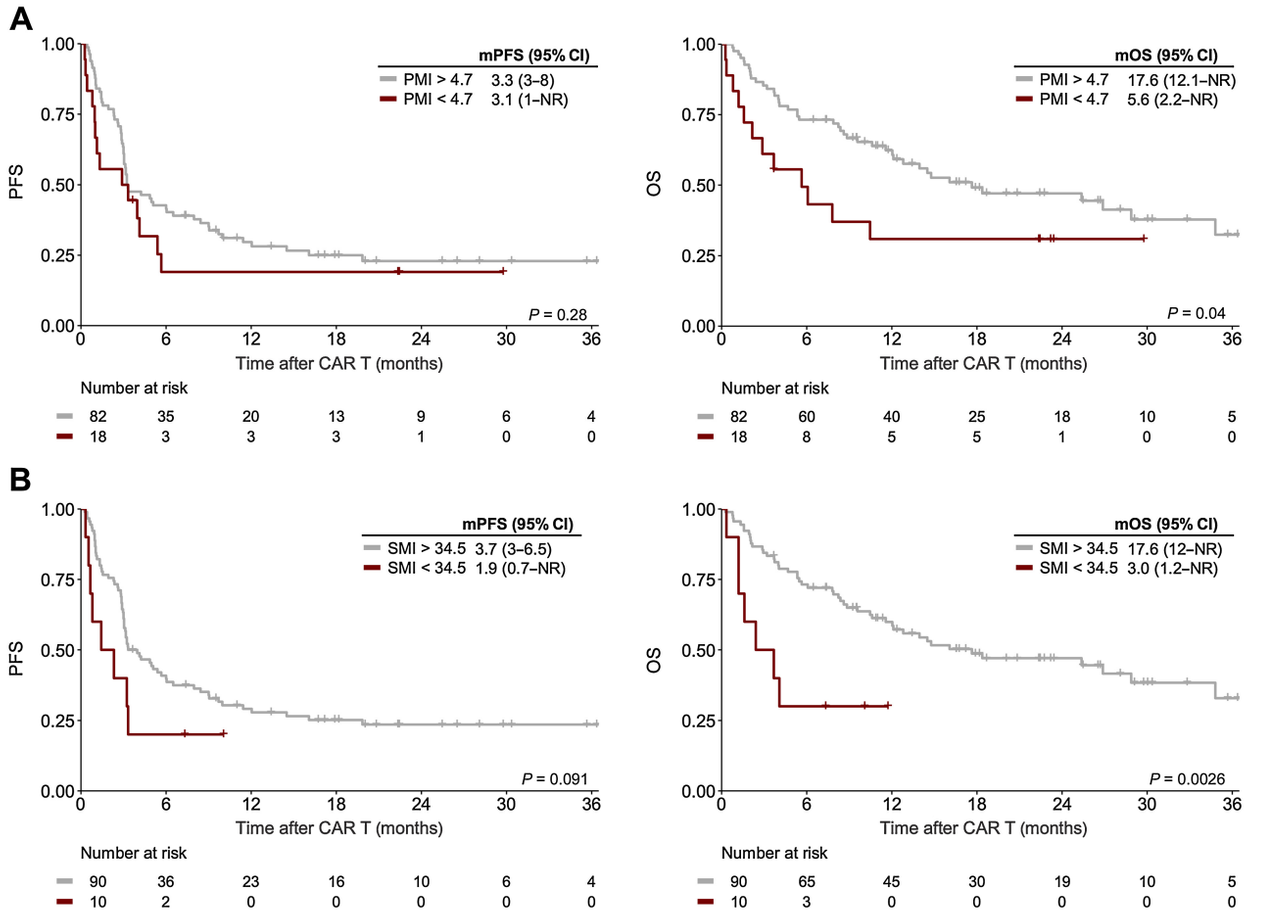

Figure 3.

Sarcopenia negatively influences post CD19.CAR-T survival outcomes. Kaplan–Meier estimates of median PFS (left) and OS (right) stratified by PMI (**A**) and SMI (**B**). The respective cutoff for each parameter and median survival in months is depicted above the graph. The *P* value of the Mantel–Cox log-rank test is denoted on the graph inset.

patients treated in the USA exhibited increased abdominal tissue deposits (Supplementary Table S6).

Sarcopenia negatively influences post CD19.CAR-T survival outcomes

Even though the sarcopenia indices (SMI/PMI) were not associated with day 90 response, sarcopenia-induced effects can be more long-lasting in nature (46). Indeed, we could establish a threshold for both lower SMI (<34.5 cm^2/m^2) and lower PMI (<4.7 cm^2/m^2), suggesting that sarcopenia may exert enduring negative effects (Supplementary Fig. S4). Although the observed differences in PFS by PMI/SMI risk group did not reach statistical significance, the deleterious impact of sarcopenia was particularly evident for OS (**Fig. 3**, right). For example, median OS was only 5.6 months in PMI^{low} patients compared with 17.6 months in PMI^{high} patients (log-rank $P = 0.04$, **Fig. 3A**). Overall survival was especially poor in the SMI^{low} risk group (mOS 3.0 months vs. 17.6 months, log-rank $P = 0.0026$, **Fig. 3B**), with a HR of 3.29 (95% CI, 1.45–7.49) for OS on univariate analysis (**Table 2**). In addition, we noted a significantly increased risk of poor OS for the PMI^{low} risk group (HR_{OS}, 1.94; 95% CI, 1.02–3.68; **Table 2**). Of interest, only a small number of patients reached the adverse risk threshold for PMI (18 patients) and SMI (10 patients).

Adverse immuno-nutritional scores represent a negative prognostic marker of post CD19.CAR-T survival outcomes

Next, we studied the prognostic influence of immuno-nutritional scores (e.g., GPS, CRP-to-albumin-ratio, PNI) on survival outcomes. The thresholds for CRP-to-albumin-ratio and PNI were identified as 1.44 and 33.5, respectively (Supplementary Fig. S4). All immuno-nutritional scores demonstrated a significant prognostic effect on univariate Cox regression (**Table 2**). CAR-T patients with a baseline GPS score ≥ 1 had markedly worse clinical outcomes compared with their GPS 0 counterparts (mPFS = 1.4 months vs. 5.0 months, log-rank $P < 0.0001$; mOS = 3.2 months vs. 28.9 months, log-rank $P < 0.0001$, **Fig. 4A**). A GPS score of 1 or greater markedly increased the risk of inferior survival (HR_{PFS}, 3.00; 95% CI, 1.81–5.00; HR_{OS}, 5.85; 95% CI, 3.26–10.52). In the case of PNI and CRP-to-albumin ratio, lower ratios also associated with poor PFS and OS (**Table 2**), and we noted a significant separation of survival curves (**Fig. 4B** and **C**). Patients with a PNI <33.5 exhibited especially adverse treatment outcomes with a mPFS and mOS of only 1.2 and 2.1 months, respectively (**Fig. 4C**).

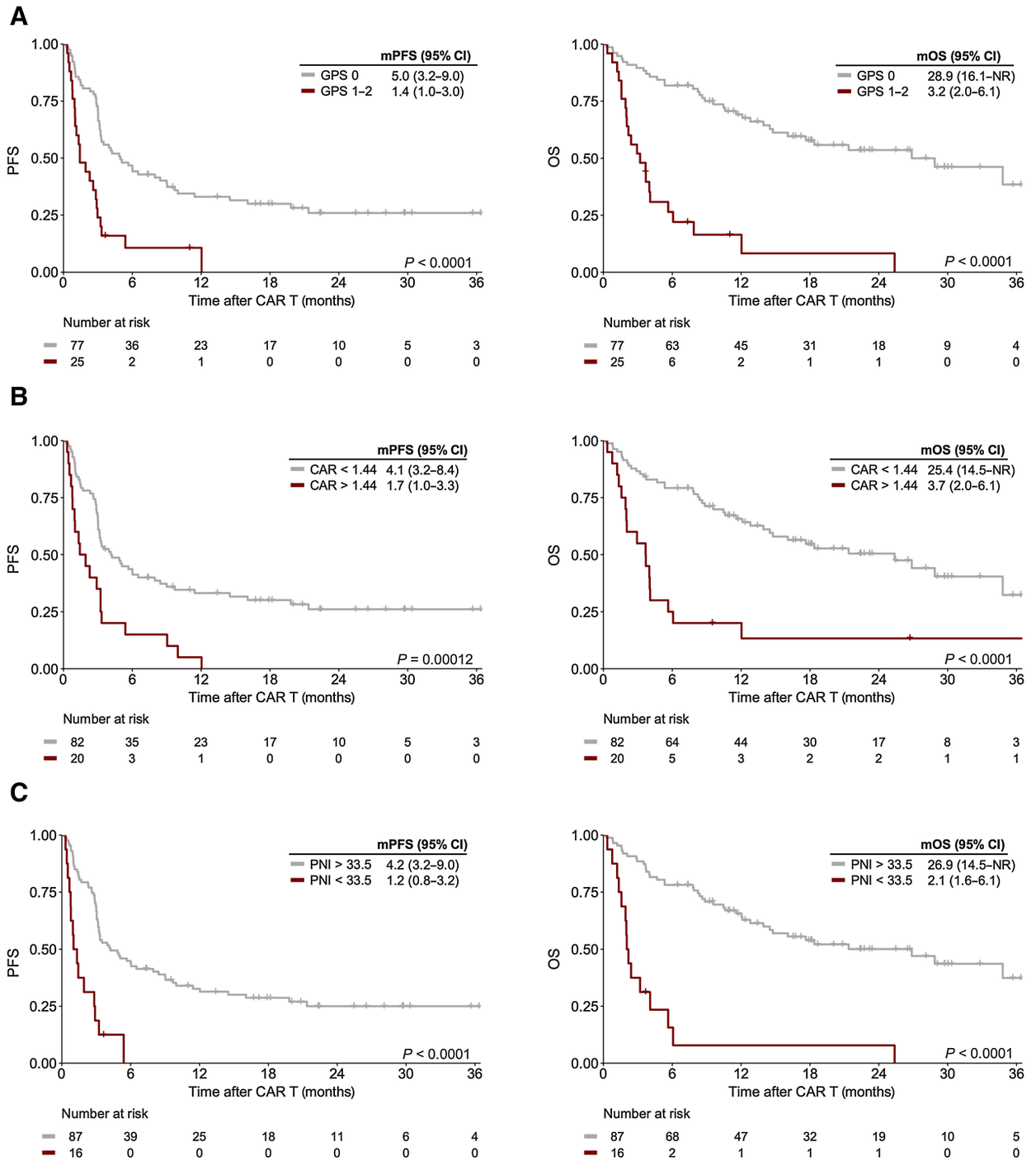

Figure 4.

Altered immuno-nutritional scores represent a negative prognostic marker of post CD19.CAR-T survival outcomes. Kaplan–Meier estimates of median PFS (left) and OS (right) stratified by GPS (**A**), CRP-to-Albumin ratio (CAR; **B**), and PNI (**C**). The respective cutoff for each parameter and median survival in months is depicted above the graph. The *P* value of the Mantel–Cox log-rank test is denoted on the graph inset.

The combination of increased muscle mass and adipose tissue is associated with excellent treatment outcomes after CD19.CAR-T

To identify the association between the different body composition features, as well as established pre–CAR T risk factors, we performed correlations between variables (**Fig. 5A**; Supplementary Fig. S5). We observed a negative correlation between PNI and serum LDH ($r = -0.328$; $P = 0.0007$) and CRP ($r = -0.432$; $P < 0.0001$) at lymphodepletion. We also observed a positive correlation between

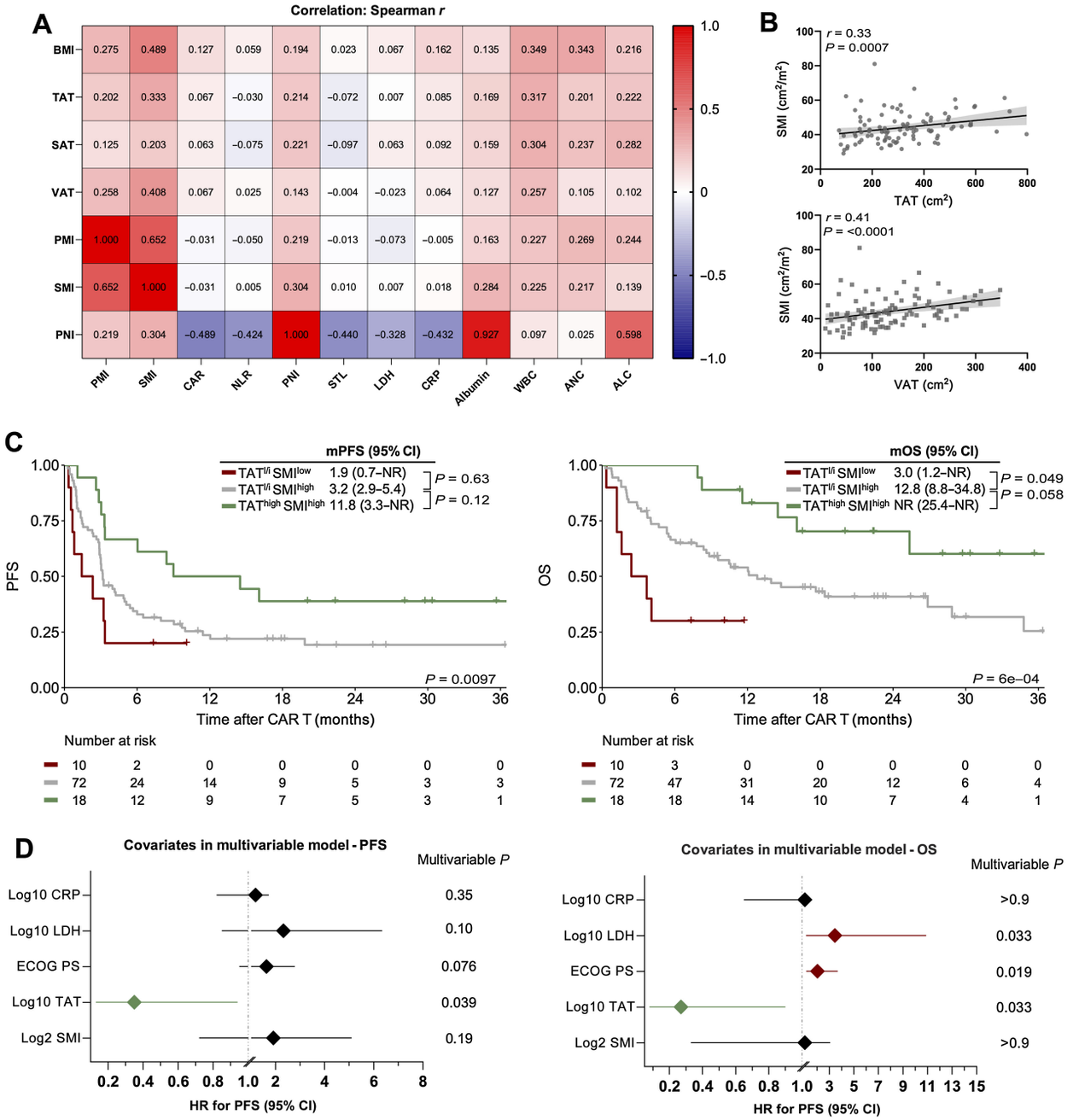

Figure 5.

The combination of increased abdominal adipose and muscle tissue is associated with excellent survival outcomes after CD19.CAR-T. **A,** A heat map displaying the correlation between body composition parameters, immuno-nutritional scores, and CAR-T risk factors. The Spearman correlation coefficient *r* is represented within the respective squares. **B,** Correlation between TAT and VAT with the amount of skeletal muscle measured by SMI. **C,** Kaplan–Meier estimates of median PFS (left) and OS (right) stratified by the combination of TAT and SMI. TAT low-intermediate (l/i) was defined as <464 cm^2 and SMI low was defined as <34.5 cm^2. The respective median survival in months is depicted above the graph. The *P* value of the Mantel–Cox log-rank test is denoted on the graph inset. **D,** Forest plots depicting multivariable Cox regression for PFS (left) and OS (right). Adjusted *P* values accounting for the respective covariates are displayed on the graph inset. Variables reaching statistical significant ($P < 0.05$) are highlighted in red (increased HR for poor survival) or green (decreased HR for poor survival). WBC, white blood cell count; ANC, absolute neutrophil count; ALC, absolute lymphocyte count.

hematopoietic function (as indicated by WBC and ANC) and increased levels of muscle mass and adipose tissue. Furthermore, we found that muscle mass and adipose tissue deposits were positively correlated (SMI vs. VAT: $r = 0.41$; $P < 0.0001$, **Fig. 5B**). To further delineate the relationship between these body composition parameters and survival outcomes, we performed a subgroup analysis for PFS and OS stratified by TAT low-to-intermediate ($TAT^{l/i}$) versus high (TAT^{high}) status and SMI risk group (SMI^{low} vs. SMI^{high}; **Fig. 5C**). Both PFS and OS were excellent in the TAT^{high}/SMI^{high} patients (1-year PFS 50%, mPFS 11.8 months; 1-year OS 83%, mOS not-reached), whereas $TAT^{l/i}/SMI^{high}$ patients exhibited intermediate treatment outcomes (1-year PFS 22%, mPFS 3.2 months; 1-year OS 51%, mOS 12.8 months). On the other hand, the combination of low muscle mass and low abdominal body fat deposits ($TAT^{l/i}/SMI^{low}$) represented a particularly adverse risk combination with a 1-year PFS and OS rate of only 20% and 30%, respectively (mPFS 1.9 months, mOS 3.0 months). Similar effects were noted upon combination of VAT and SMI (Supplementary Fig. S6). Taken together, these data underline that the combination of high abdominal fat and muscle mass represents an auspicious combination for patients undergoing CD19.CAR-T, whereas low muscle and adipose tissue reserves portend poor treatment outcomes.

Multivariable analysis

To understand if the body composition features TAT and SMI were impacted by other established prognostic risk factors, we performed multivariable Cox proportional hazards modeling for both PFS and OS. The model was adjusted for the covariates LDH, CRP, and ECOG performance status, which were associated with poor survival outcomes in our patient cohort (**Table 2**), and are of high clinical relevance in the context of CD19.CAR-T as surrogate markers of inflammation and tumor burden (6, 7, 9, 10). The sum of target lesions (STL) was excluded because measurements were not available in ≥100 patients and a high degree of collinearity was observed with serum LDH ($r = 0.57$; $P < 0.001$). Notably, TAT was retained as an independent positive prognostic marker risk for both PFS and OS in the multivariable model (**Fig. 5D**; Supplementary Table S4). For example, higher TAT levels reduced the risk of inferior PFS (adjusted HR, 0.35; 95% CI, 0.13–0.94) and OS (aHR, 0.27; 95% CI, 0.08–0.90). Conversely, sarcopenia, as indicated by a low SMI, was not retained as an independent adverse prognostic marker in the multivariable models (**Fig. 5D**). When PNI, comprised of albumin and total lymphocyte count, was introduced into the multivariable model (Supplementary Table S5), we noted that higher PNI scores were independently associated with favorable treatment outcomes (aHR_{PFS}, 0.07; 95% CI, 0.02–0.26; aHR_{OS}, 0.05; 95% CI, 0.01–0.20).

Discussion

In this single-center observational study of 106 patients receiving CD19.CAR-T for R/R B-cell malignancies in a real-world setting, we report a first-of-its-kind analysis of the prognostic influence of CT-based body composition in the context of CAR T-cell therapy. We demonstrate that increased abdominal fat, sarcopenia, and poor nutritional status impact survival outcomes.

The fact that increased abdominal fat deposits were independently associated with superior PFS/OS suggests that the obesity paradox may extend to patients receiving modern T cell–based immunotherapies. Our CT-based body composition analyses enable the precise characterization of the prognostic influence of the different adipose tissue deposits, with our analysis demonstrating a particularly dominant effect of (visceral) abdominal fat. Importantly, the consideration of anthropometric features alone likely only paints a partial picture of the role that adipose tissue plays as a host-dependent factor. Both BMI and waist circumference were not significantly correlated with clinical outcomes in our analysis, which is consistent with a previous study that did not observe a significant prognostic impact of BMI in patients receiving axicabtagene ciloleucel (22). On the one hand, this may argue against the hypothesis that body composition-driven effects on survival are primarily mediated by pharmacokinetic interactions between adipose tissue and the dosing of Flu/Cy lymphodepletion or the CAR T-cells themselves. On the other hand, multiple studies modeling the pharmacokinetics/-dynamics of fludarabine demonstrated that weight and renal function (rather than BMI or BSA) represent the best predictors of fludarabine exposure (47–49). Adipose tissue may also exert pro-immunogenic anti-lymphoma effects via metaflammation (50). We have previously demonstrated that VAT^{high} patients exhibit both earlier and more severe CRS (25). These clinical observations were accompanied by markedly increased peak IL6 levels and a shorter time to peak IL6, findings that are consistent with previous reports delineating a mechanism of IL6 secretion by adipocytes and adipose-tissue macrophages (51–53). These findings may also explain the high sensitivity of (visceral) abdominal fat, which is particularly relevant for metaflammation processes (54). Future translational studies will have to elucidate if these effects are driven by systemic inflammation alone, or if VAT^{high} patients may also observe more pronounced CAR T-cell expansion.

Sarcopenia has long been considered to have a deleterious effect on the antitumor responses of cancer therapies in general (55) and immunotherapy in particular (56). Interestingly, we observed a differential influence of sarcopenia in regards to 90-day response versus long-term survival outcomes. This may indicate that adipose tissue is more immunogenic than muscle tissue in the short-term, whereas sarcopenia rather exerts long-lasting adverse effects. Low muscle mass is associated with poor tolerance of anticancer therapy, increased treatment-related complications, and prolonged hospitalization (57, 58). Furthermore, low muscle mass generally represents a read-out of inadequate functional reserve (56). Lower overall survival in SMI^{low} patients may therefore reflect an inability to receive efficacious post-relapse therapy and/or enter clinical trials. Still, a recent publication demonstrated a negative impact of poor functional status in the context of CD19.CAR-T as early as day 90, although this study incorporated weight- and serum-based markers of cachexia as opposed to CT-based quantification of muscle tissue distribution and did not perform multivariable analyses (59). In any case, sarcopenia likely represents a useful marker of general fitness in patients presenting to CAR T-cell therapy.

We further demonstrated that immuno-nutritional scores were associated with adverse survival outcomes (e.g., GPS, CRP-to-albumin ratio, PNI). The poor survival outcomes in PNI^{low} patients highlight the relevance of both hypoalbuminemia and lymphopenia as potential risk factors for long-term survival after CD19.CAR-T, which is also in line with a recently published report by Roy and colleagues (59). The PNI represents one of the most broadly studied parameters for nutritional status in patients with lymphoma and was shown to have a prognostic role for survival outcomes in a variety of NHL entities in both the pre- and postrituximab era (60–62). Moreover, prior reports have also outlined roles for the absolute lymphocyte count (including the unique kinetics after CAR-T transfusion; refs. 63, 64) and hypoalbuminemia in the context of CD19.CAR-T

specifically (65), further highlighting the utility of the PNI in the CAR-T era. Because the PNI incorporates readily available laboratory parameters and is easy-to-assess, future prognostic models may integrate the score as a component of multimodal risk assessment. Of interest, we noted significantly increased muscle (e.g., PMI, SMI) and adipose tissue deposits (e.g., BMI, TAT, SAT, VAT) as well as higher PNI values in the patients from the US cohort (Supplementary Table S6), all of which represented positive prognostic markers in our analysis. This not only provides context for the slightly more favorable treatment outcomes in our US cohort, but also underlines the variety of host factors that may contribute to survival differences by geographic region (66). Still, this observation may have been influenced by other baseline factors, such as prior treatment lines and use of CAR product (Supplementary Table S7).

This study has several relevant limitations. It was retrospective and limited to a moderate number of patients receiving CD19.CAR-T for R/R LBCL, raising concerns for potential overfitting. Metabolic tumor volume (MTV), waist circumference, and epicardial adipose tissue (EAT) measurements were not available for all the patients in the cohort. Although the main study results were affirmed across two separate health care systems with distinct patient populations (USA and Germany), the results of the present study need to be prospectively validated in larger patient cohorts across multiple health care systems and institutions. A prerequisite will be standardization and harmonization of the assessment of adipose and muscle tissue distributions across different centers considering the specialized software that was employed in this study. Still, these proof-of-concept findings are hypothesis-generating and warrant further systematic analysis. If confirmed prospectively, we see several useful clinical applications. First, our results highlight the importance of measures to prevent sarcopenia and malnutrition, which can include physical therapy and dietary consultation while patients are admitted to the hospital, as well as specialized rehabilitation measures after discharge. This may also represent an added benefit of outpatient CAR T-cell therapy, which could prevent long phases of immobilization while in the hospital (67). At the same time, the short time intervals between T-cell apheresis and CAR-T treatment, which often incorporate phases of intensive bridging therapy due to the nature of aggressive lymphoma, may impede the ability of "prehab" (i.e., pretreatment rehab) to facilitate large improvements in functional capacity. Concomitantly, such interventions need to be considered as early as possible during the natural course of disease, ideally at time of initial diagnosis. Second, future interventional studies may compare the impact of physical exercise and diet on patient-reported outcomes. The role of diet in particular remains poorly understood and may impact the composition of the gut microbiome, with recent evidence pointing towards the multifunctional and immunomodulatory role of the microbiome in the context of CAR-T (12). Finally, future radiology reports of patients presenting to CD19.CAR-T may not only read out measures of the underlying lymphoma (e.g., MTV, SUV_{max}), but also host-dependent factors as outlined in this study.

In conclusion, these data provide evidence for an adverse prognostic role of sarcopenia and malnutrition in the context of CD19.CAR-T, while increased visceral fat deposits were associated with superior survival outcomes. Our findings highlight the critical role of the host in determining treatment response, and invite future translational research studying the underlying mechanisms of the immunometabolic impact of body composition.

Authors' Disclosures

K. Rejeski reports grants and personal fees from Kite/Gilead and personal fees from Novartis outside the submitted work. D.M. Cordas dos Santos reports other support from German Cancer Consortium (DKTK) and grants from Ludwig-Maximilians-University during the conduct of the study. V.L. Bücklein reports personal fees from Amgen, Pfizer, and Novartis; grants from BMS/Celgene; grants and personal fees from Kite/Gilead outside the submitted work. V. Blumenberg reports grants and other support from Gilead/Kite, Janssen, and Novartis; grants from BMS, Roche, and Takeda outside the submitted work. C. Schmidt reports personal fees from BMS and AstraZeneca; nonfinancial support from Kite Gilead; personal fees and nonfinancial support from Johnson & Johnson outside the submitted work. W.G. Kunz reports personal fees from Bristol Myers Squibb and Mint Medical outside the submitted work. M.D. Jain reports grants and personal fees from Kite/Gilead, personal fees from MyeloidTx, and grants from Incyte outside the submitted work. S. Theurich reports grants from DFG (German Research Organisation), LMU University Hospital Munich, and German Translational Cancer Research Consortium (DKTK) during the conduct of the study; other support from Kyowa Kirin, Janssen, Pfizer, Takeda, Sanofi, GSK, BMS/Celgene, and from Amgen outside the submitted work. M. Subklewe reports grants from DFG, DFG, BZKF, and DKTK during the conduct of the study; personal fees from Novartis, Janssen, Amgen, Celgene/BMS, and Kite/Gilead; grants from Seattle Genetics outside the submitted work. No disclosures were reported by the other authors.

Authors' Contributions

K. Rejeski: Conceptualization, resources, data curation, software, formal analysis, investigation, visualization, methodology, writing–original draft. **D.M. Cordas dos Santos:** Conceptualization, data curation, software, formal analysis, investigation, visualization, methodology, writing–original draft. **N.H. Parker:** Investigation. **V.L. Bücklein:** Formal analysis, investigation. **M. Winkelmann:** Formal analysis, investigation. **K.S. Jhaveri:** Investigation. **L. Liu:** Formal analysis, investigation. **P. Trinkner:** Formal analysis, investigation. **S. Günther:** Formal analysis, investigation. **P. Karschnia:** Formal analysis, investigation. **V. Blumenberg:** Formal analysis, investigation. **C. Schmidt:** Formal analysis, investigation. **W.G. Kunz:** Formal analysis, investigation. **M. von Bergwelt-Baildon:** Formal analysis, investigation. **M.D. Jain:** Investigation, writing–review and editing. **S. Theurich:** Conceptualization, resources, supervision, funding acquisition, project administration, writing–review and editing. **M. Subklewe:** Conceptualization, resources, supervision, funding acquisition, writing–original draft, project administration.

Acknowledgments

K. Rejeski, D.M. Cordas dos Santos, and V. Blumenberg received a fellowship from the School of Oncology of the German Cancer Consortium (DKTK). D.M. Cordas dos Santos, P. Trinkner, and S. Günther received funding from the Medical Faculty of the Ludwig-Maximilians-University in Munich, Germany. K. Rejeski, V. Blumenberg, and V.L. Bücklein were funded by the Else Kröner Forschungskolleg (EKFK) within the Munich Clinician Scientist Program (MCSP). This work was supported by a Deutsche Forschungsgemeinschaft (DFG, German Research Foundation) research grant provided within the Sonderforschungbereich SFB-TRR 388/1 2021 – 452881907 (to M. Subklewe and S. Theurich), and DFG research grant 451580403 (to M. Subklewe). The work was further supported by the Bavarian Elite Graduate Training Network (to M. Subklewe), the Wilhelm-Sander Stiftung (to M. Subklewe, project no. 2018.087.1), the Else-Kröner-Fresenius Stiftung (to M. Subklewe), and the Bavarian Cancer Research Center (BZKF). We are grateful for the support of all patients and the personnel of the LMU University Hospital who supported this work.

The publication costs of this article were defrayed in part by the payment of publication fees. Therefore, and solely to indicate this fact, this article is hereby marked "advertisement" in accordance with 18 USC section 1734.

Note

Supplementary data for this article are available at Cancer Immunology Research Online (http://cancerimmunolres.aacrjournals.org/).

Received June 15, 2022; revised December 6, 2022; accepted April 5, 2023; published first April 11, 2023.

References

1. Locke FL, Ghobadi A, Jacobson CA, Miklos DB, Lekakis LJ, Oluwole OO, et al. Long-term safety and activity of axicabtagene ciloleucel in refractory large B-cell lymphoma (ZUMA-1): a single-arm, multicentre, phase 1–2 trial. Lancet Oncol 2019;20:31–42.
2. Schuster SJ, Bishop MR, Tam CS, Waller EK, Borchmann P, McGuirk JP, et al. Tisagenlecleucel in adult relapsed or refractory diffuse large B-cell lymphoma. N Engl J Med 2019;380:45–56.
3. Locke FL, Miklos DB, Jacobson CA, Perales M-A, Kersten M-J, Oluwole OO, et al. Axicabtagene ciloleucel as second-line therapy for large B-cell lymphoma. N Engl J Med 2022;386:640–54.
4. Wang M, Munoz J, Goy A, Locke FL, Jacobson CA, Hill BT, et al. KTE-X19 CAR T-cell therapy in relapsed or refractory mantle-cell lymphoma. N Engl J Med 2020;382:1331–42.
5. Iacoboni G, Rejeski K, Villacampa G, van Doesum JA, Chiappella A, Bonifazi F, et al. Real-world evidence of brexucabtagene autoleucel for the treatment of relapsed or refractory mantle cell lymphoma. Blood Adv 2022;6:3606–10.
6. Bethge WA, Martus P, Schmitt M, Holtick U, Subklewe M, von Tresckow B, et al. GLA/DRST real-world outcome analysis of CAR-T cell therapies for large B-cell lymphoma in Germany. Blood 2022;140:349–58.
7. Nastoupil LJ, Jain MD, Feng L, Spiegel JY, Ghobadi A, Lin Y, et al. Standard-of-care axicabtagene ciloleucel for relapsed or refractory large B-cell lymphoma: results from the US lymphoma CAR T consortium. J Clin Oncol 2020;38:3119–28.
8. Sterner RC, Sterner RM. CAR-T cell therapy: current limitations and potential strategies. Blood Cancer J 2021;11:69.
9. Locke FL, Rossi JM, Neelapu SS, Jacobson CA, Miklos DB, Ghobadi A, et al. Tumor burden, inflammation, and product attributes determine outcomes of axicabtagene ciloleucel in large B-cell lymphoma. Blood Adv 2020;4:4898–911.
10. Jain MD, Zhao H, Wang X, Atkins R, Menges M, Reid K, et al. Tumor interferon signaling and suppressive myeloid cells are associated with CAR T-cell failure in large B-cell lymphoma. Blood 2021;137:2621–33.
11. Rejeski K, Perez A, Sesques P, Hoster E, Berger C, Jentzsch L, et al. CAR-HEMATOTOX: A model for CAR T-cell related hematological toxicity in relapsed/refractory large B-cell lymphoma. Blood 2021;138:2499–513.
12. Smith M, Dai A, Ghilardi G, Amelsberg KV, Devlin SM, Pajarillo R, et al. Gut microbiome correlates of response and toxicity following anti-CD19 CAR T cell therapy. Nat Med 2022;28:713–23.
13. Rejeski K, Perez A, Iacoboni G, Penack O, Bücklein V, Jentzsch L, et al. The CAR-HEMATOTOX risk-stratifies patients for severe infections and disease progression after CD19 CAR-T in R/R LBCL. J Immunother Cancer 2022;10:e004475.
14. Wang LS, Murphy CT, Ruth K, Zaorsky NG, Smaldone MC, Sobczak ML, et al. Impact of obesity on outcomes after definitive dose-escalated intensity-modulated radiotherapy for localized prostate cancer. Cancer 2015;121:3010–7.
15. Cai B, Li K, Li G. Impact of obesity on major surgical outcomes in ovarian cancer: a meta-analysis. Front Oncol 2022;12:841306.
16. Lee DH, Giovannucci EL. The obesity paradox in cancer: epidemiologic insights and perspectives. Curr Nutr Rep 2019;8:175–81.
17. Trestini I, Caldart A, Dodi A, Avancini A, Tregnago D, Sartori G, et al. Body composition as a modulator of response to immunotherapy in lung cancer: time to deal with it. ESMO Open 2021;6:100095.
18. Cortellini A, Ricciuti B, Tiseo M, Bria E, Banna GL, Aerts JG, et al. Baseline BMI and BMI variation during first line pembrolizumab in NSCLC patients with a PD-L1 expression >/= 50%: a multicenter study with external validation. J Immunother Cancer 2020;8:e001403.
19. Rogado J, Sánchez-Torres JM, Romero-Laorden N, Ballesteros AI, Pacheco-Barcia V, Ramos-Leví A, et al. Immune-related adverse events predict the therapeutic efficacy of anti-PD-1 antibodies in cancer patients. Eur J Cancer 2019;109:21–27.
20. Stevenson JKR, Qiao Y, Chan KKW, Beca J, Isaranuwatchai W, Guo H, et al. Improved survival in overweight and obese patients with aggressive B-cell lymphoma treated with rituximab-containing chemotherapy for curative intent. Leuk Lymphoma 2019;60:1399–408.
21. Scheich S, Enßle JC, Mücke VT, Acker F, Aspacher L, Wolf S, et al. Obesity is associated with an impaired survival in lymphoma patients undergoing autologous stem cell transplantation. PLoS One 2019;14:e0225035.
22. Wudhikarn K, Bansal R, Khurana A, Hathcock MA, Bennani NN, Paludo J, et al. The impact of obesity and body weight on the outcome of patients with relapsed/refractory large B-cell lymphoma treated with axicabtagene ciloleucel. Blood Cancer J 2021;11:124.
23. Ferrante AW Jr. The immune cells in adipose tissue. Diabetes Obes Metab 2013;15 Suppl 3:34–8.
24. Ibrahim MM. Subcutaneous and visceral adipose tissue: structural and functional differences. Obes Rev 2010;11:11–8.
25. Dos Santos DMC, Rejeski K, Winkelmann M, Liu L, Trinkner P, Günther S, et al. Increased visceral fat distribution and body composition impact cytokine release syndrome onset and severity after CD19 CAR-T in advanced B-cell malignancies. Haematologica 2022;107:2096–107.
26. Peterson SJ, Mozer M. Differentiating sarcopenia and cachexia among patients with cancer. Nutr Clin Pract 2017;32:30–39.
27. Nelke C, Dziewas R, Minnerup J, Meuth SG, Ruck T. Skeletal muscle as potential central link between sarcopenia and immune senescence. EBioMedicine 2019;49:381–8.
28. Rogeri PS, Gasparini SO, Martins GL, Costa LKF, Araujo CC, Lugaresi R, et al. Crosstalk between skeletal muscle and immune system: which roles do IL-6 and glutamine play? Front Physiol 2020;11:582258.
29. Giudice J, Taylor JM. Muscle as a paracrine and endocrine organ. Curr Opin Pharmacol 2017;34:49–55.
30. Conlon KC, Lugli E, Welles HC, Rosenberg SA, Fojo AT, Morris JC, et al. Redistribution, hyperproliferation, activation of natural killer cells and CD8 T cells, and cytokine production during first-in-human clinical trial of recombinant human interleukin-15 in patients with cancer. J Clin Oncol 2015;33:74–82.
31. Proctor MJ, Morrison DS, Talwar D, Balmer SM, O'Reilly DSJ, Foulis AK, et al. An inflammation-based prognostic score (mGPS) predicts cancer survival independent of tumour site: a glasgow inflammation outcome study. Br J Cancer 2011;104:726–34.
32. Nozoe T, Iguchi T, Egashira A, Adachi E, Matsukuma A, Ezaki T. Significance of modified Glasgow prognostic score as a useful indicator for prognosis of patients with gastric carcinoma. Am J Surg 2011;201:186–91.
33. Jung J, Lee H, Heo JY, Chang MH, Lee E, Park WS, et al. High level of pre-treatment C-reactive protein to albumin ratio predicts inferior prognosis in diffuse large B-cell lymphoma. Sci Rep 2021;11:2674.
34. Luan C, Wang F, Wei N, Chen B. Prognostic nutritional index and the prognosis of diffuse large b-cell lymphoma: a meta-analysis. Cancer Cell Int 2020;20:455.
35. Mu S, Ai L, Fan F, Qin Y, Sun C, Hu Y. Prognostic role of neutrophil-to-lymphocyte ratio in diffuse large B cell lymphoma patients: an updated dose-response meta-analysis. Cancer Cell Int 2018;18:119.
36. Pennisi M, Sanchez-Escamilla M, Flynn JR, Shouval R, Alarcon Tomas A, Silverberg ML, et al. Modified-EASIX predicts severe cytokine release syndrome and neurotoxicity after chimeric antigen receptor (CAR) T cells. Blood Adv 2021;5:3397–406.
37. Greenbaum U, Strati P, Saliba RM, Torres J, Rondon G, Nieto Y, et al. CRP and ferritin in addition to the EASIX score predict CAR-T-related toxicity. Blood Adv 2021;5:2799–806.
38. Xu X, Gnanaprakasam JNR, Sherman J, Wang R. A metabolism toolbox for CAR T therapy. Front Oncol 2019;9:322.
39. Lee DW, Santomasso BD, Locke FL, Ghobadi A, Turtle CJ, Brudno JN, et al. ASTCT consensus grading for cytokine release syndrome and neurologic toxicity associated with immune effector cells. Biol Blood Marrow Transplant 2019;25:625–38.
40. Gomez-Perez SL, Haus JM, Sheean P, Patel B, Mar W, Chaudhry V, et al. Measuring abdominal circumference and skeletal muscle from a single cross-sectional computed tomography image: a step-by-step guide for clinicians using national institutes of Health ImageJ. JPEN J Parenter Enteral Nutr 2016;40:308–18.
41. Prado CMM, Baracos VE, McCargar LJ, Mourtzakis M, Mulder KE, Reiman T, et al. Body composition as an independent determinant of 5-fluorouracil-based chemotherapy toxicity. Clin Cancer Res 2007;13:3264–8.
42. Jayawardena E, Li D, Nakanishi R, Dey D, Dailing C, Qureshi A, et al. Non-contrast cardiac CT-based quantitative evaluation of epicardial and intra-thoracic fat in healthy, recently menopausal women: reproducibility data from the kronos early estrogen prevention study. J Cardiovasc Comput Tomogr 2020;14:55–59.
43. Cheson BD, Fisher RI, Barrington SF, Cavalli F, Schwartz LH, Zucca E, et al. Recommendations for initial evaluation, staging, and response assessment of Hodgkin and non-Hodgkin lymphoma: the Lugano classification. J Clin Oncol 2014;32:3059–68.
44. Kuhnl A, Roddie C, Kirkwood AA, Menne T, Cuadrado M, Marzolini MAV, et al. Early FDG-PET response predicts CAR-T failure in large B-cell lymphoma. Blood Adv 2022;6:321–6.

45. Budczies J, Klauschen F, Sinn BV, Győrffy B, Schmitt WD, Darb-Esfahani S, et al. Cutoff Finder: a comprehensive and straightforward Web application enabling rapid biomarker cutoff optimization. PLoS One 2012;7:e51862.
46. Veronese N, Koyanagi A, Cereda E, Maggi S, Barbagallo M, Dominguez LJ, et al. Sarcopenia reduces quality of life in the long-term: longitudinal analyses from the English longitudinal study of ageing. Eur Geriatr Med 2022;13:633–9.
47. Ivaturi V, Dvorak CC, Chan D, Liu T, Cowan MJ, Wahlstrom J, et al. Pharmacokinetics and model-based dosing to optimize fludarabine therapy in pediatric hematopoietic cell transplant recipients. Biol Blood Marrow Transplant 2017;23:1701–13.
48. Langenhorst JB, Dorlo TPC, van Maarseveen EM, Nierkens S, Kuball J, Boelens JJ, et al. Population pharmacokinetics of fludarabine in children and adults during conditioning prior to allogeneic hematopoietic cell transplantation. Clin Pharmacokinet 2019;58:627–37.
49. Dekker L, Calkoen FG, Jiang Y, Blok H, Veldkamp SR, De Koning C, et al. Fludarabine exposure predicts outcome after CD19 CAR T-cell therapy in children and young adults with acute leukemia. Blood Adv 2022;6:1969–76.
50. Hotamisligil GS. Inflammation, metaflammation and immunometabolic disorders. Nature 2017;542:177–85.
51. Eder K, Baffy N, Falus A, Fulop AK. The major inflammatory mediator interleukin-6 and obesity. Inflamm Res 2009;58:727–36.
52. Roytblat L, Rachinsky M, Fisher A, Greemberg L, Shapira Y, Douvdevani A, et al. Raised interleukin-6 levels in obese patients. Obes Res 2000;8:673–5.
53. Fain JN, Madan AK, Hiler ML, Cheema P, Bahouth SW. Comparison of the release of adipokines by adipose tissue, adipose tissue matrix, and adipocytes from visceral and subcutaneous abdominal adipose tissues of obese humans. Endocrinology 2004;145:2273–82.
54. Wang L, Sun P, Wu Y, Wang L. Metabolic tissue-resident CD8(+) T cells: a key player in obesity-related diseases. Obes Rev 2021;22:e13133.
55. Shachar SS, Williams GR, Muss HB, Nishijima TF. Prognostic value of sarcopenia in adults with solid tumours: a meta-analysis and systematic review. Eur J Cancer 2016;57:58–67.
56. Li S, Wang T, Tong G, Li X, You D, Cong M. Prognostic impact of sarcopenia on clinical outcomes in malignancies treated with immune checkpoint inhibitors: a systematic review and meta-analysis. Front Oncol 2021;11:726257.
57. Shachar SS, Deal AM, Weinberg M, Nyrop KA, Williams GR, Nishijima TF, et al. Skeletal muscle measures as predictors of toxicity, hospitalization, and survival in patients with metastatic breast cancer receiving taxane-based chemotherapy. Clin Cancer Res 2017;23:658–65.
58. Shachar SS, Deal AM, Weinberg M, Williams GR, Nyrop KA, Popuri K, et al. Body composition as a predictor of toxicity in patients receiving anthracycline and taxane-based chemotherapy for early-stage breast cancer. Clin Cancer Res 2017;23:3537–43.
59. Roy I, Smilnak G, Burkart M, Hamilton E, Thorp K, Miyata S, et al. Cachexia is a risk factor for negative clinical and functional outcomes in patients receiving chimeric antigen receptor T-cell therapy for B-cell non-Hodgkin lymphoma. Br J Haematol 2022;197:71–75.
60. Zhou Q, Wei Y, Huang F, Wei X, Wei Q, Hao X, et al. Low prognostic nutritional index predicts poor outcome in diffuse large B-cell lymphoma treated with R-CHOP. Int J Hematol 2016;104:485–90.
61. Go S-I, Park S, Kang MH, Kim H-G, Kim HR, Lee G-W. Clinical impact of prognostic nutritional index in diffuse large B cell lymphoma. Ann Hematol 2019;98:401–11.
62. Chen K-L, Liu Y-H, Li W-Y, Chen J, Gu Y-K, Geng Q-R, et al. The prognostic nutritional index predicts survival for patients with extranodal natural killer/T cell lymphoma, nasal type. Ann Hematol 2015;94:1389–400.
63. Liu Y, Chen W, Yu M, Li H, Cheng H, Cao J, et al. Absolute lymphocyte count prior to lymphodepletion impacts outcomes in multiple myeloma patients treated with chimeric antigen receptor T cells. Transplant Cell Ther 2022;28:118.e1–5.
64. Faude S, Wei J, Muralidharan K, Xu X, Wertheim G, Paessler M, et al. Absolute lymphocyte count proliferation kinetics after CAR T-cell infusion impact response and relapse. Blood Adv 2021;5:2128–36.
65. Vercellino L, Di Blasi R, Kanoun S, Tessoulin B, Rossi C, D'Aveni-Piney M, et al. Predictive factors of early progression after CAR T-cell therapy in relapsed/refractory diffuse large B-cell lymphoma. Blood Adv 2020;4:5607–15.
66. Bücklein V, Perez A, Iacoboni G, Rejeski K, Holtick U, Penack O, et al. P1447: inferior outcomes of Eu Vs. Us patients with relapsed/refractory large B-cell lymphoma after Cd19 Car T-cell therapy are impacted by baseline risk factors and car product choice. Hemasphere 2022;6:1330–1. eCollection 2022 Jun.
67. Myers GD, Verneris MR, Goy A, Maziarz RT. Perspectives on outpatient administration of CAR-T cell therapy in aggressive B-cell lymphoma and acute lymphoblastic leukemia. J Immunother Cancer 2021;9:e002056.